BOREAL ENVIRONMENT RESEARCH 26: 61–77
ISSN 1797-2469 (online)

Helsinki 29 April 2021

Application of an ice thermodynamic model to a shallow freshwater lagoon

Rasa Idzelytė[1)*] and Georg Umgiesser[2)1)]

[1)] *Marine Research Institute, Klaipėda University, Universiteto ave. 17, 92294, Klaipėda, Lithuania (*corresponding author's e-mail: rasa.idzelyte@apc.ku.lt)*
[2)] *CNR — National Research Council of Italy, ISMAR — Institute of Marine Sciences, Castello 2737/f, 30122, Venice, Italy*

Received 3 Sep. 2020, final version received 26 Mar. 2021, accepted 29 Mar. 2021

Idzelytė R. & Umgiesser G. 2021: Application of an ice thermodynamic model to a shallow freshwater lagoon. *Boreal Env. Res.* 26: 61–77.

In this study, we apply an ice thermodynamic model to a shallow freshwater lagoon in the south-eastern part of the Baltic Sea — the Curonian Lagoon. The model results were compared with the measurement data from three near-shore stations during the period of 2004–2017. The simulation data showed the model to be capable of replicating ice thickness dynamics rather well (mean R = 0.92, RMSE = 6 cm). Although the model overestimated the number of ice days (NID) on average by one month (ranging from 3 to 40 days), the overall pattern was very similar to observations (R = 0.95). We further assessed the ice thickness and NID projections in the near (2021–2040) and far (2081–2100) future under two climate change scenarios (RCP4.5 and RCP8.5). The results showed that the mean (max) ice thickness could decrease by 10–49% (6–34%) in the near and 41–75% (22–55%) in the far future under RCP4.5, and by 2–52% (2–30%) in the near and 75–88% (50–71%) in the far future under RCP8.5 compared to the baseline period of 1986–2005. The NID will shorten by 9–19% (9–22%) in the near and 15–36% (46–57%) in the far future under RCP4.5 (RCP8.5) scenarios, compared with the baseline period.

Introduction

Many places in the world are experiencing extreme events of precipitation or droughts, rising water level and air temperature, changing ice phenology (Fallis 2018, IPCC 2019). The latter, ice, is an important and early indicator of climate change for which accurate sea ice cover observations are needed. As it is already evident in the polar regions (Stroeve *et al.* 2012, Yadav *et al.* 2020), the reduction of the Arctic sea ice can accelerate global warming in the long run (Wunderling *et al.* 2020), and weather extremes in the northern hemisphere (Börgel *et al.* 2020, Simon *et al.* 2020).

Sea ice has been of high interest for studies in the Baltic Sea region, where its systematic observations started in the 19th century (Jevrejeva *et al.* 2004). During that period, navigation was the main motivation for sea ice observations; whilst nowadays, the interest in climate change impact is increasing (HELCOM 2013). Although the maximum sea ice extent, thickness, season duration and its severity in the Baltic Sea has a large interannual variability, the decreasing trend of it has accelerated since the 1980s (Vihma and Haapala

Editor in charge of this article: Kai Myrberg

2009, Haapala *et al.* 2015) and future modelling projections under different climate change scenarios reveal that this pattern will persist (Luomaranta *et al.* 2014). These changes are largely determined by the atmospheric circulation processes in the North Atlantic, such as North Atlantic Oscillation (Girjatowicz 2005, Yu Karpechko *et al.* 2015, Kļaviņš *et al.* 2016, Idzelytė *et al.* 2019). It is clear that climate change will modify ice characteristics in the future and numerical modelling can evaluate the magnitude of it.

The importance of ice in the polar regions to the global climate, e.g., oceanic and atmospheric circulation (Vihma 2014, Pedersen *et al.* 2016), has led to a progressive large-scale modelling of the sea ice. Global climate models are capable of reproducing the observed present and past climate variations and are suitable for making plausible projections of its future changes by taking into account different climate change scenarios (Randall *et al.* 2007). As global modelling results often do not describe adequately small scales, local scale model applications are needed for better representation of ice parameters.

Freshwater ice phenology is driven by solar radiation, snow accumulation on top of its surface, and mostly by the air temperature (George 2010), which is increasing worldwide (IPCC 2019). The ice season in the northern temperate lakes shortens at a rate of 7 to 17 days per century (EEA 2017), the future projections estimate a similar reduction rate (Sharma *et al.* 2019). Since the formation of sea ice is a very fast process governed mainly by the exchange of heat at the air-water interface and mixing characteristics, along with the overall capacity of the water body to store the heat (Martin and McCutcheon 1999), the smaller and shallower domains tend to freeze faster, due to a much smaller water volume underneath the ice cover.

Although real knowledge comes from studying ice in situ, it is often expensive, complicated, and in many cases dangerous to do winter field sampling campaigns. Numerical modelling is a good tool for assessing the changing processes in the water body. It not only helps filling in the gaps in observational data, but also projects future states of the studied object, e.g., the formation and evolution of ice (Peng *et al.* 2020). Three processes have to be taken into account to model the ice cover: thermodynamic processes, dynamic processes, and the processes that couple these two components (Chassignet and Verron 1998, Hunke *et al.* 2011). Modelling studies of Baltic Sea ice are extensive (Vihma and Haapala 2009), ranging from simulations of thermodynamic ice growth in the fast ice zones along the coast (Tedesco *et al.* 2009) to ridging in the drift zones needing combination of both thermodynamic and dynamic processes (Leppäranta and Myrberg 2009, Herman *et al.* 2011, Pemberton *et al.* 2017, Jakacki and Meler 2019).

Since many of the physical and ecological processes depend on ice thickness, in this paper we focus on ice thermodynamics only, disregarding the variability of ice thickness due to the dynamic processes of ice rafting and ridging. The Curonian Lagoon (Fig. 1) is a large but shallow freshwater body (greatest natural depth: 5.8 m, mean depth: 3.8 m, area: ~1600 km^2) in the southeastern part of the Baltic Sea, connected to it by a narrow strait. The lagoon is influenced by freshwater input from the rivers (mainly from the Nemunas River) and saline water from the sea. During strong northerly winds, the saltwater intrusion events affect the northern part of the lagoon (Zemlys *et al.* 2013). The increase of salinity, shorter water residence time compared to the rest of the lagoon (Umgiesser *et al.* 2016, Idzelytė *et al.* 2020), and the overall turbid characteristics of this area lead to a shorter ice cover season (Idzelytė *et al.* 2019).

In this study, to complement the recent statistical models (Jakimavičius *et al.* 2019) with new methods, we present a case study of deterministic ice thermodynamic model application for the simulation of ice cover thickness in the Curonian Lagoon. Although the numerical description of this lagoon is attracting more interest, this study is a new approach on estimating ice thickness. We evaluated the suitability of calibrated and validated model for other modelling studies and applications for this freshwater environment. Further, since the recreational activities, e.g., ice fishing, during the ice cover season in the Curonian Lagoon are of high relevance, we apply the model to investigate the ice cover response to different climate change scenarios and compare with already present knowledge regarding the Curonian Lagoon and the Baltic Sea region.

Material and methods

Ice in the Curonian Lagoon

Historical ice thickness data (Baukšys 1978) show that during the beginning of the second half of the 20th century, every winter, a 10–70 cm thick ice cover formed in the lagoon. The ice measurements in the lagoon have been taken every season since then, however, comparing with the magnitude of sea ice research in the Baltic Sea, the investigation of ice cover (thickness, extent, duration, and their dynamics) in the Curonian Lagoon (CL) has not been undertaken properly. Only in recent years has this type of research emerged, e.g., a study of remote sensing data evaluating the variability of ice cover extent, phenology, and season dynamics (Idzelytė *et al.* 2019). It revealed that in many cases the satellite data perform better compared to the conventional in situ measurements for defining the ice cover phenology. Furthermore, the spatially detailed data of ice season duration allowed indication of locations where the ice remains the longest/shortest. Likewise, it revealed that the overall ice duration is closely linked to the air temperature. However, this study did not assess ice thickness. Another study by Kozlov *et al.* (2020) revealed that satellite products of ice thickness perform rather well for the periods of gradual ice growth, although in case of rapid growth it is underestimated by 20–50%.

Two other studies were based on statistical methods. The first investigated the dependency of ice cover formation on changes in air temperature, water surface temperature, and salinity by comparing multivariate linear regression and regression kriging methods, of which latter showed better performance (Rukšėnienė *et al.* 2015). However, here, the correlation of the results with observational data was very low, and ice thickness was not addressed separately. The second study looked at future projections of different ice indices, including thickness, using statistical methods and regression analysis in the scope of different climate change scenarios (Jakimavičius *et al*. 2019), called representative concentration pathways (RCPs). Those are greenhouse gas concentration trajectories adopted by the Intergovernmental Panel on Climate Change (IPCC)

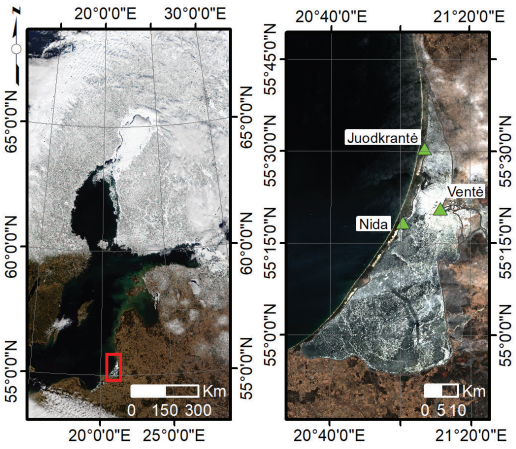

Fig 1. Location of the Curonian Lagoon (right) with respect to the Baltic Sea (left). Green triangles indicate the location of coastal ice observation stations. Image of the Baltic Sea provided by the MODIS Rapid Response team (taken from https://visibleearth.nasa.gov/), image of the Curonian Lagoon acquired from the Copernicus Sentinel-2B mission (taken from https://scihub.copernicus.eu/).

and identified by their approximate total radiative forcing in year 2100 relative to year 1750: 2.6 W m^{-2} for RCP2.6 (limits the increase of global mean temperature to 2°C, called mitigation scenario), 4.5 W m^{-2} for RCP4.5 (stabilizes radiative forcing at 4.5 W m^{-2} in the year 2100 without ever exceeding it, called stabilization scenario), and 8.5 W m^{-2} for RCP8.5 (continuously growing greenhouse gas emissions, called "business as usual" scenario) (IPCC, 2013). Jakimavičius *et al.* (2019) concluded that the annual mean ice thickness in the CL by the end of this century could decline to 13 cm (under RCP 2.6), or 9 cm (under RCP4.5), or even form only once every five years reaching 4–11 cm thickness (under RCP8.5). Statistical models perform very well if the predictors do not change, although if they would, the model cannot project the studied parameters accurately, thus in this article we explore the deterministic ice thermodynamic model results.

Data

The input data required for model calibration consists of cloud cover, downward shortwave radiation, precipitation rate, specific humidity,

air temperature, and wind speed. We obtained these data for the period of 2004–2017 from ERA5 — the fifth generation ECMWF (European Centre for Medium-Range Weather Forecasts) reanalysis for the global climate and weather hourly data on single levels, available in the Climate Data Store developed by the Copernicus Climate Change Service (C3S) at the ECMWF (Hersbach *et al.* 2018).

We validated the model output data with snow and ice thickness observation data in three coastal stations (Nida, Juodkrantė, and Ventė; Fig. 1) provided by Marine Research Department of the Environment Protection Agency (MRD of EPA) of Lithuania. The observation data covered the whole study period in Nida and Ventė, however in Juodkrantė ice observation program was discontinued in 2012.

For the analysis of climate change impact on ice thickness, we acquired the meteorological data from CORDEX (Coordinated Regional Downscaling Experiment) scenarios for Europe from the Rossby Centre regional climate model (RCA4), which consisted of five sets of simulations (downscaling) driven by the following five global climate models: EC-Earth (ICHEC), CNRM-CM5 (CNRM), IPSL-CM5A-MR (IPSL), HadGEM2-ES (MOHC), and MPI-ESM-LR (MPI). These datasets spanned a period from 1970 to 2100, divided in two parts, one from 1970 to 2005 (baseline, BS), and one from 2006 to 2100 (future), according to two Representative Concentration Pathway (RCP) scenarios: RCP4.5 — stabilization scenario, and RCP8.5 — "business as usual" scenario (IPCC 2013).

MRD of EPA of Lithuania provided the air temperature measurement data in all three stations (Nida, Juodkrantė, and Ventė; Fig. 1), and Lithuanian Hydrometeorological Service provided the precipitation measurement data, however measurements were taken only in Nida.

Ice thermodynamic model

Here, we used the improved version of the enhanced sea-ice thermodynamic model ESIM2 by Tedesco *et al.* (2010). The first version of this 0D model was already applied for studying landfast sea ice in four different areas of the Baltic Sea (Tedesco *et al.* 2009). This application showed that model is capable to adequately represent the growth, decay, and overall seasonal changes of the ice, meteoric ice (h_{mi}, consisting of snow ice and superimposed ice), and snow thickness.

The prognostic variables of ESIM2 are three layers of snow and three layers of ice (Fig. 2, Table 1). Snow thickness (h_s) in the model consists of new fallen snow ($(h_s)_n$), "bucket snow" ($(h_s)_{bk}$) — initial snowfall collected in a virtual bucked, which after fully filled is emptied, and snow is compacted ($(h_s)_{cp}$). Ice layers consist of snow ice (h_{si}), superimposed ice (h_{ss}), and sea ice (h_i). The model initiates snow ice formation every time the ice draft exceeded the thickness of the ice. If the melted snow is in contact with the layer of ice, then it refreezes and superimposed ice forms. Finally, sea ice is divided into two layers: biologically active ($(h_i)_{bio}$) and biologically inactive ($(h_i)_{abio}$). The latter two were added for the model to be capable of simulating salinity evolution in sea ice and to be compatible with the biogeochemical flux model (Tedesco *et al.* 2010). Since the Curonian Lagoon is considered mainly freshwater, salinity is set to be constant and equal to zero (Table 1).

The model also simulates temperature at the surface and at the interface of each snow and ice layer. Melting is initiated every time when the surface temperature is at the melting point, while the rate of it depends on the net heat flux balance between the surface (sensible, F_{SE}, latent, F_{LA}, shortwave, F_{SW}, and longwave radiation, F_{LW}) and conductive (F_C) fluxes (Fig. 2).The heat flux from water to the bottom of the ice (oceanic heat flux, F_W) in previous model applications (Tedesco *et al.* 2009, 2010) was represented by a constant value, for our study, we incorporated a bulk formulation by Omstedt and Wettlaufer (1992):

$$F_W = \rho_w C_p C_h \Delta U (T_\infty - T_F), \quad (1)$$

where C_p is specific heat of water, C_h — heat transfer coefficient, ΔU is the relative velocity between the ice drift and the current at a reference level (we consider it to be constant and equal to 0.05 m s^{-1}), T_∞ — mixed layer

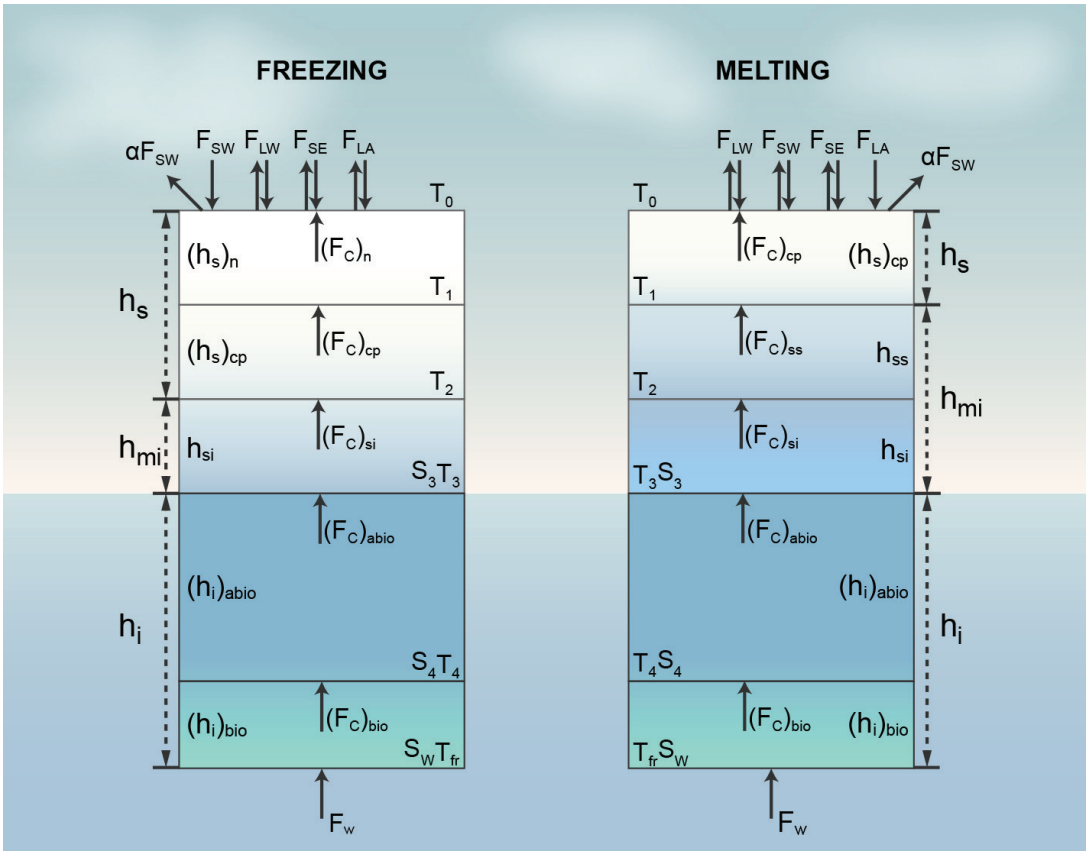

Fig 2. Schematic representation of the ice thermodynamic model structure during the freezing and melting periods (adapted from Tedesco 2009).

temperature, and T_F — freezing temperature. Since the Curonian Lagoon is shallow and has a well-mixed water column, the water temperature beneath the ice is mostly equal to the freezing temperature throughout the ice cover season, which results in $F_W \approx 0$ W m^{-2}.

In order to properly simulate the ice freeze onset and melt-off, the ice thermodynamic model is coupled with a slab ocean model, which is an approximation of the ocean mixed layer. During ice-free periods, this slab ocean model computes a temperature of the mixed

Table 1. Ice thermodynamic model parameters that differ from Tedesco et al. (2009; 2010).

Parameter	Value	Unit
Mixed layer depth, h_{mix}	1.5	m
Water density, ρ_w	1000	kg m^{-3}
Water salinity, S_w	0.0	g/kg
Snow precipitation density, $(\rho_s)_{prec}$	300	kg m^{-3}
Density of cold new snow, $(\rho_s)_y$	300	kg m^{-3}
Density of warm new snow, $(\rho_s)_y$	350	kg m^{-3}
Density of cold "bucket" snow, $(\rho_s)_{bk}$	350	kg m^{-3}
Density of warm "bucket" snow, $(\rho_s)_{bk}$	400	kg m^{-3}
Density of cold compacted snow, $(\rho_s)_{cp}$	350	kg m^{-3}
Density of warm compacted snow, $(\rho_s)_{cp}$	400	kg m^{-3}

layer based on the depth and surface energy fluxes.

Simulations' set-up and scenarios

We carried out several simulations for the model calibration and sensitivity using different snow density values. However in this study, only two types of simulations are presented: 1) with the original model set-up as described in Tedesco *et al.* (2010) (hereafter $\mathrm{Pres_{Orig}}$), and 2) with increased densities of all snow types by 50 kg m^{-3} (hereafter $\mathrm{Pres}_{\rho s}$) (Table 2). We ran the ice model for each of the three stations (Fig. 1) for the period of 2004–2017, with a one-hour model time step, and selected the best model set-up by evaluating the root-mean-square error (RMSE) and Pearson correlation coefficient (R) between measured and observed values of the ice thickness.

We also compared freeze onset (FO) and melt-off (MO) dates derived from coastal observations ($\mathrm{FO_O}$ and $\mathrm{MO_O}$) with the ones of the ice model, by computing the difference in days. The latter we analysed in two parts: 1) the date of first (last) ice, $\mathrm{FO_M}$ ($\mathrm{MO_M}$), and 2) the date of first (last) ice before (after) the continuous ice cover, $\mathrm{FO_{M_{corr}}}$ ($\mathrm{MO_{M_{corr}}}$), this way eliminating the sporadic very thin ice formation events before and after the continuous ice season. Additionally, we compared the total number of ice days (NID), denoting the exact period that ice was observed in the coastal stations and computed by the model.

To investigate the sensitivity of ice model to the air temperature and precipitation rate, we set-up a test case of one ice season in Nida during 2011–2012 when the model gave the best results compared with observation data. For this, we ran the ice thermodynamic model increasing air temperature by 2°, 4°, and 6°C, and decreasing it by 1° and 2°C, as well as increasing and decreasing the precipitation rate by 50% and 100% at every time step. The mean snow and ice thickness were computed for the Nov.–Apr. period, as well as the maximum thickness and number of ice and snow days.

To compute the climate change impact on ice thickness, we used input data from five climate models: CNRM, ICHEC, IPSL, MOHC, and MPI averaged over three points in the lagoon (Nida, Juodkrantė, and Ventė; Fig. 1). For the climate change simulations, we shortened the baseline period starting from 1986 (as suggested in IPCC, 2019) and divided the future period in two sections for near and far future for both RCP scenarios (Table 2).

Since air temperature and precipitation data from the ERA5 and climate models have bias comparing to the observations, we corrected it. The air temperature was corrected (T_{BC}) by simply adding the difference between the observed, T_{O}, and modelled average air temperature, $\overline{T}_{\mathrm{M}}$, respectively (Lenderink *et al.* 2007):

$$T_{\mathrm{BC}}(t) = T_{\mathrm{M}}(t) + \left(\overline{T}_{\mathrm{O}} - \overline{T}_{\mathrm{M}}\right). \quad (2)$$

Precipitation ($\mathrm{PR_{BC}}$) was corrected by multiplying the ratio between the observed ($\mathrm{PR_O}$) and modelled ($\mathrm{PR_M}$) values:

$$\mathrm{PR_{BC}}(t) = \mathrm{PR_M}(t)\frac{\overline{\mathrm{PR_O}}}{\overline{\mathrm{PR_M}}}, \quad (3)$$

Table 2. Summary of the simulations.

Name	Period	Description
$\mathrm{Pres_{Orig}}$	2004–2017	Present-day period with original model set-up as described in Tedesco et al. (2010)
$\mathrm{Pres}_{\rho s}$	2004–2017	Present-day period with increased densities of all snow types by 50 kg m^{-3}
BS	1986–2005	Baseline period
$\mathrm{RCP4.5_{near}}$	2021–2040	RCP4.5 scenario in the near future
$\mathrm{RCP4.5_{far}}$	2081–2100	RCP4.5 scenario in the far future
$\mathrm{RCP8.5_{near}}$	2021–2040	RCP8.5 scenario in the near future
$\mathrm{RCP8.5_{far}}$	2081–2100	RCP8.5 scenario in the far future

$\overline{T}_O$, $\overline{T}_M$, $\overline{PR}_O$, and $\overline{PR}_M$ were computed for the period of Nov.–Apr. of 1993–2005, for which the observation data were available. The bias correction was applied for both — baseline and future datasets. The scenario runs were corrected based on the bias from the corresponding baseline period datasets.

We compared the future projections with the BS by computing the average and maximum ice thickness and number of ice days for the period of Nov.–Apr. of each winter season. The future change was evaluated by computing a percentage of change from the baseline period. The trend significance of the ice thickness during the baseline (1986–2005) and the whole future period (2006–2100) under RCP4.5 and RCP8.5 scenarios was evaluated using the Mann-Kendall test at a 0.05 significance level with a 95% confidence level (Kendall and Gibbons 1990). We evaluated the decrease rate by taking the slope parameter from linear regression equation generated for the same periods.

Results

Model calibration and validation

We calibrated the model by testing several density values of all snow types. The statistics of the results (Table 3) showed that the model achieved the best results when using increased densities of all snow types by 50 kg m^{-3}, $Pres_{\rho S}$, in contrast to the original model set-up described in Tedesco *et al.* (2010). This was especially true for the station in Nida, for which both the air temperature and precipitation ERA5 data were corrected with the measurements, thus the ice model gave higher correlation coefficient values not only for the ice, but for snow thickness as well.

The comparison of ice model results and observations from the coastal stations (Fig. 3) showed that the model largely underestimated snow thickness in all three stations. Although, the overall snow growth pattern in Ventė is moderate, in Nida and Juodkrantė the correlation is strong. Nonetheless, the model described the ice thickness formation and evolution very well (Fig. 4), and in all three stations correlation with the measurement data is high (R is 0.92, 0.96 and 0.89 in Nida, Juodkrantė, and Ventė, respectively).

The average difference of freeze onset dates (Table 4) revealed that in the model initial ice formation (FO_M) started very early, which was not recorded in the coastal stations (FO_O). There usually were very short freezing events with ice thickness in a matter of millimetres, this way leading to a very large initial freeze onset difference. The model data fit the observations much better with eliminated sporadic freezing events in the beginning of the ice season ($FO_{M_{corr}}$). The same was with melt-off dates (Table 4); here in many cases, the model still indicated ice presence, although it was already not visible in the coastal stations.

The model overestimated the total number of ice days (NID) in all three stations (Fig. 4) by more than one month in Nida and Juodkrantė, and 19 days in Ventė. Nonetheless, the overall pattern of NID was very similar to that of coastal observations, having a very strong correlation (three station mean R = 0.95). The elimination of short thin ice formation events in the beginning and occasionally at the end of the ice season revealed an even higher correlation with the observed ice duration (three station mean R = 0.98), while the RMSE decreased by 10 days.

Table 3. Calibration statistics of ice and snow thickness. Model set-up types ($Pres_{Orig}$ and $Pres_{\rho S}$) are described in the section Simulations' set-up and scenarios. RMSE values are in meters.

		Nida		Juodkrantė		Ventė	
		$Pres_{Orig}$	$Pres_{\rho S}$	$Pres_{Orig}$	$Pres_{\rho S}$	$Pres_{Orig}$	$Pres_{\rho S}$
Ice	*R*	0.89	0.92	0.95	0.96	0.87	0.89
	RMSE	0.08	0.07	0.06	0.04	0.06	0.06
Snow	*R*	0.69	0.73	0.62	0.63	0.56	0.56
	RMSE	0.05	0.05	0.07	0.07	0.04	0.04

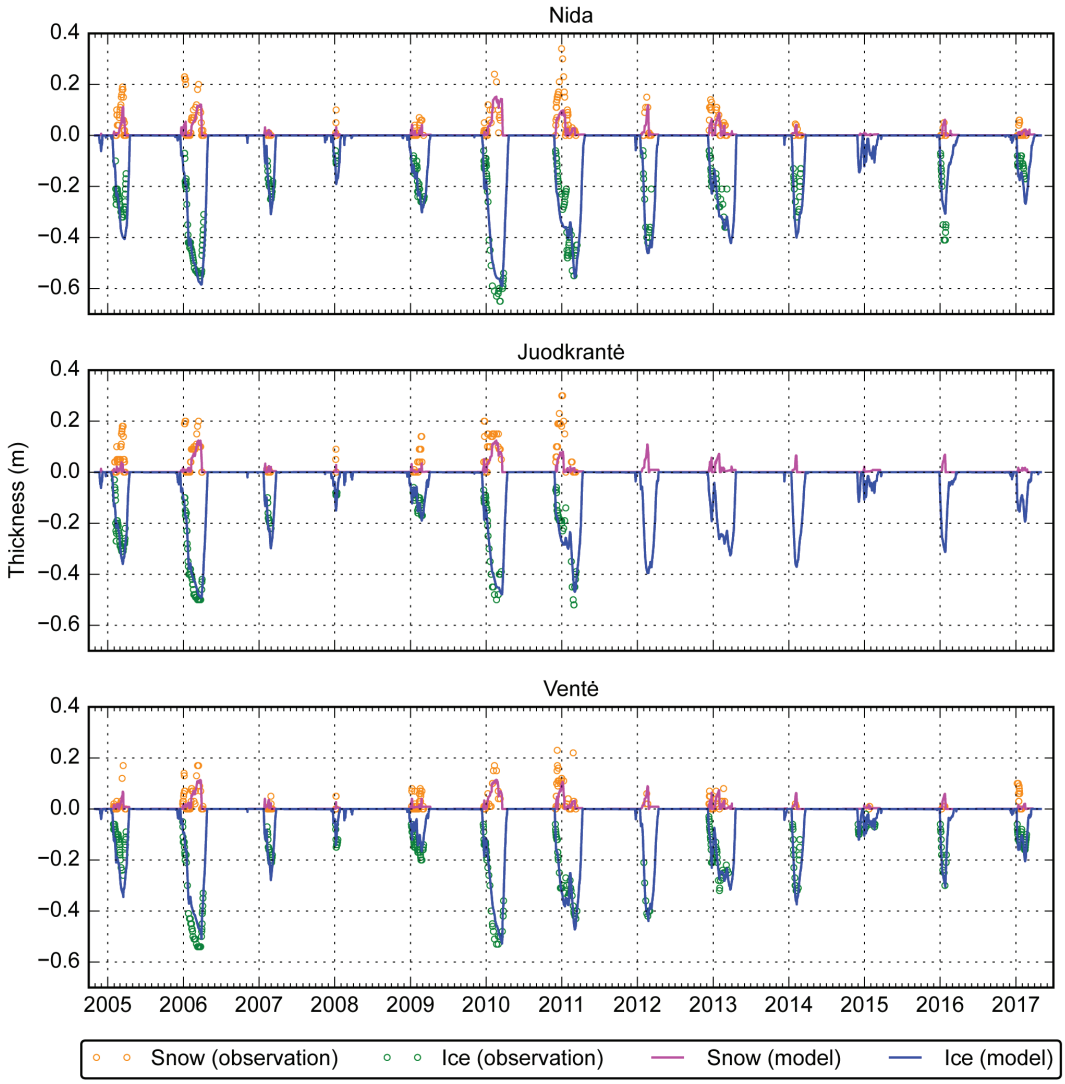

Fig 3. Observations and modelled snow and ice cover thickness in three coastal stations: Nida, Juodkrantė, and Ventė in 2004–2017. Snow and ice thickness layers are grouped together in two groups: snow — positive ordinate, and ice — negative ordinate.

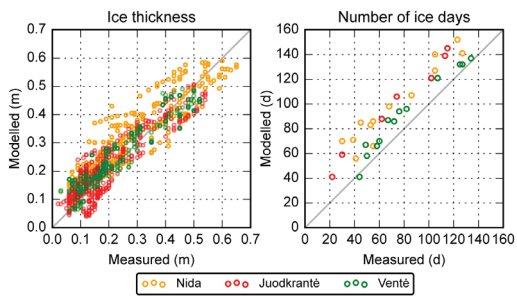

Fig 4. Scatterplots of measured and modelled ice thickness and a number of ice days in Nida, Juodkrantė, and Ventė for the period 2004–2017.

Sensitivity to air temperature and precipitation rate

During the 2011–2012 winter season in Nida, the model produced very good ice ($R = 0.94$) and snow ($R = 0.90$) thickness results, allowing to test the model sensitivity to air temperature and precipitation rate changes in a controlled environment. The results using increased air temperature showed that the average ice thickness decreased by 2 cm/°C, while the maximum ice thickness decreased by 3 cm/°C (Fig. 5). Higher

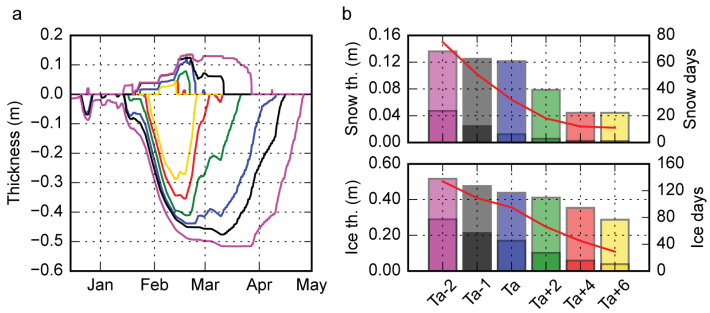

Fig 5. Ice and snow thickness sensitivity due to varying air temperature: in (**a**) Nida during 2011–2012, computed using measured air temperature (Ta, blue), increased by 2°C (Ta+2, green), 4°C (Ta+4, red), and 6°C (Ta+6, yellow), and decreased by 1°C (Ta–1, black) and 2°C (Ta–2, purple); and (**b**) Ice (upper panel) and snow thickness (lower panel) of each air temperature change. Light colour indicates maximum and dark colour average thickness (labelled at the left axis). Also inserted is the red line, labelled on the right, indicating the number of ice and snow days. Average values were computed for a five-month period (Dec. 2011–May 2012).

air temperatures did not have a considerable impact on the average snow thickness, although the maximum of it decreased by 1 cm/°C. The number of ice days decreased by 11 days/°C and snow days by 4 days/°C. The decreasing temperature results showed that the average ice thickness increased by 6 cm/°C, while the maximum ice thickness increased by 4 cm/°C. The maximum snow thickness increased only by 1 cm/°C, while the average by 2 cm/°C. The overall number of ice days increased by 28 and snow by 22 days/°C.

The model is less sensitive to the changes in precipitation rate compared to air temperature. Decreased precipitation rate led to likewise decreased snow thickness (Fig. 6), although while increased rate did not have major effects on the maximum snow thickness and number of days, it increased the average thickness. A precipitation rate decrease of 50% led to 4 cm higher maximum ice thickness, and to 5 cm higher when there was no precipitation. Increased precipitation rate by 50% (100%) led to a maximum ice thickness decrease by 2 cm (3 cm). The increased precipitation rate did not have major effects on overall number of snow days, while number of ice days slightly decreased. The decreased precipitation rate likewise reduces the number of snow days, although the number of ice days stayed the same.

Climate change

The average Nov.–Apr. air temperature during the 1993–2005 period was higher in all climate model datasets by ~1.3°C compared with the measurements, apart from CNRM, which had the most similar air temperature data — the difference being only ~0.16°C. The average Nov.–Apr. air temperature during the baseline period of CNRM, ICHEC, and IPSL climate

Table 4. The difference of freeze onset (melt-off) dates between observation, FO_O (MO_O), and modelling, FO_M (MO_M) and $FO_{M_{corr}}$ ($MO_{M_{corr}}$), data in three coastal stations. Dash indicates subtraction. Negative numbers indicate that ice thermodynamic model produced ice data longer than it was recorded in the coastal stations.

	Nida			Juodkrantė			Ventė		
	mean	min	max	mean	min	max	mean	min	max
FO_O–FO_M	27	1	81	28	1	66	17	1	63
FO_O–$FO_{M_{corr}}$	4	0	13	5	1	12	3	0	9
MO_O–MO_M	–21	–39	–12	–20	–31	–9	–10	–19	–5
MO_O–$MO_{M_{corr}}$	–20	–39	–6	–15	–25	–3	–10	–19	–5

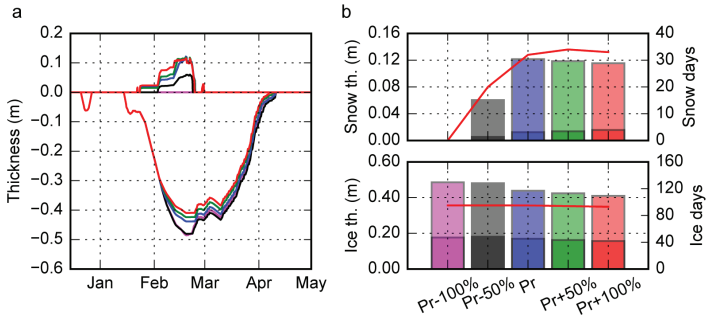

Fig 6. Ice and snow thickness sensitivity due to varying precipitation rate: in (**a**) Nida during 2011–2012, computed using measured precipitation rate (Pr, blue), increased by 50% (Pr+50, green), 100% (Pr+100, red), and decreased by 50%°C (Pr–50, black) and 100% (Pr–100, purple); and (**b**) Ice (upper panel) and snow thickness (lower panel) of each precipitation rate change. Light colour indicates maximum and dark colour average thickness (labelled at the left axis). Also inserted is the red line, labelled on the right, indicating the number of ice and snow days. Average values were computed for five-month period (Dec. 2011–May 2012).

model data was lower compared to the present-day period, while for MOHC and MPI it was higher (Fig. 7), which all became lower compared to the present-day period after the bias correction, and the model produced better results. The precipitation rate was close to the observations, apart from ICHEC and IPSL datasets, having slightly larger values.

The mean ice thickness (averaged over Nov.–Apr.) in the near future, derived using ICHEC, IPSL, and MOHC model data showed a large decrease compared to the baseline period (Table 5), while the model that fit the observations the best (CNRM) showed a mean ice thickness decrease by 10.4–12.7%. The highest change was in the far future, when mean ice thickness decreased by 41–75% under $RCP4.5_{far}$ and 75–88% under $RCP8.5_{far}$. The maximum ice thickness is likely to steadily decrease throughout the century (Fig. 8). In the near future it is not likely to change drastically, by 6–34% under $RCP4.5_{near}$ and 2–30% under $RCP8.5_{near}$,

Table 5. Percentage of a decrease of mean and maximum ice thickness and number of ice days (NID) in the near (2021–2040) and far (2081–2100) future compared to the baseline period (1986–2005) under different climate change scenarios of data from five climate models: ICHEC, CNRM, IPSL, MOHC, and MPI.

	CNRM	ICHEC	IPSL	MOHC	MPI
Mean					
$RCP4.5_{near}$	10.4	39.3	49.0	33.9	27.1
$RCP8.5_{near}$	12.7	52.4	36.5	31.3	1.7
$RCP4.5_{far}$	68.6	59.7	74.5	54.2	40.7
$RCP8.5_{far}$	85.9	88.2	87.8	85.8	75.4
Max					
$RCP4.5_{near}$	6.3	13.9	33.7	24.9	13.6
$RCP8.5_{near}$	2.8	29.6	17.6	13.5	1.8
$RCP4.5_{far}$	45.5	30.9	55.2	40.7	22.3
$RCP8.5_{far}$	60.3	60.2	71.4	64.0	50.3
NID					
$RCP4.5_{near}$	8.5	12.4	19.3	16.2	17.7
$RCP8.5_{near}$	8.7	21.9	11.5	18.3	17.6
$RCP4.5_{far}$	35.5	34.7	29.9	31.4	15.5
$RCP8.5_{far}$	55.7	60.2	67.0	57.3	46.0

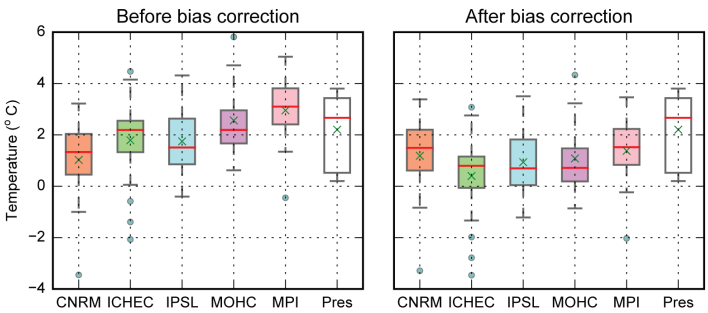

Fig 7. Average Nov–Apr. air temperature during the baseline (1986–2005) period of data from five climate models: ICHEC, CNRM, IPSL, MOHC, and MPI, compared with the present-day period (Pres, 2004–2017). Circles denote the outliers, red line indicate the median, and green "*x*" is the mean. Please note that the bias correction was done using the available observation data for the period of 1993–2005.

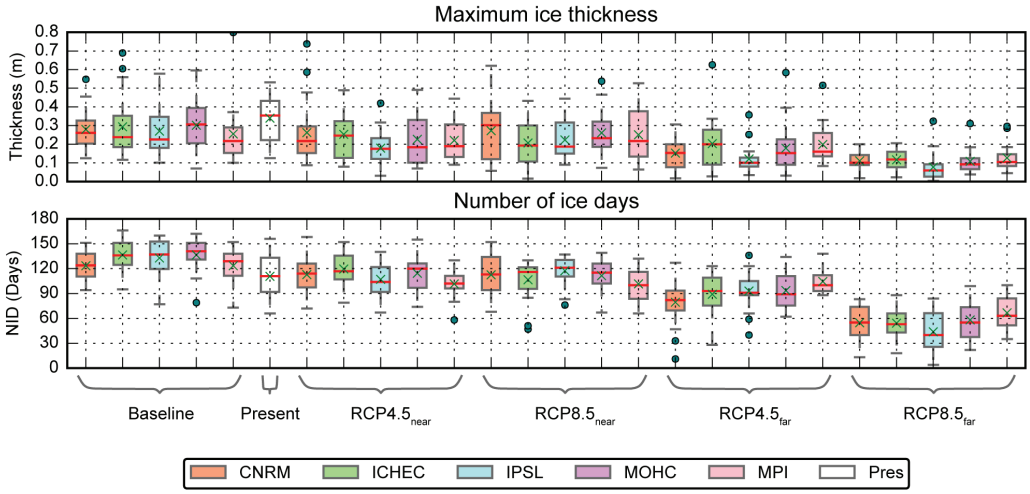

Fig 8. Maximum ice thickness and number of ice days during the baseline (1986–2006), present (2004–2017), near (2021–2040) and far (2081–2100) future periods under RCP4.5 and RCP8.5 scenarios using data from five climate models: ICHEC, CNRM, IPSL, MOHC, and MPI. Circles denote the outliers, red line indicate the median, and green "*x*" is the mean.

although in the far future it could decrease by 22–55% and 50–71% under RCP4.5$_{far}$ and RCP8.5$_{far}$ respectively (Table 5).

The ice thickness distribution (Fig. 9) shows that the five-model mean/max ice thickness was 9/20 cm during the baseline period. In the near future mean thickness could decrease to 6 cm under both RCP scenarios, and the maximum thickness could decrease to 15 cm under RCP4.5$_{near}$ and 16 cm under RCP8.5$_{near}$. In the far future, mean/max ice thickness could reach 4/9 cm under RCP4.5$_{far}$ and 1/4cm under RCP8.5$_{far}$.

The mean and maximum ice thickness from all the models over the 2006–2100 period display statistically significant decreasing trend ($p < 0.05$), while the trends during the baseline period were not significant. During the baseline period mean/max ice thickness was decreasing with 0.30–0.91/0.63–1.32 cm year^{-1}, while MOHC and MPI showed an increasing rate of 0.09/0.36 and 0.34/0.79 cm year^{-1}, respectively (Table 6). The decreasing tendency of mean/max ice thickness varied from 0.04–0.07/0.11–0.18 cm year^{-1} under RCP4.5 and 0.05–0.12/0.11–0.30 cm year^{-1} under RCP8.5 climate change scenarios.

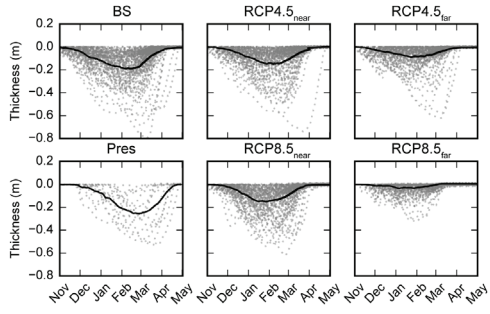

Fig 9. Ice thickness during the baseline (BS, 1986–2005), present (Pres, 2004–2017), and near (2021–2040) and far (2081–2100) future periods under RCP4.5 and RCP8.5 scenarios using data from five climate models: ICHEC, CNRM, IPSL, MOHC, and MPI. Black line is the average thickness of all models.

The decreasing number of ice days (NID) pattern is similar to that of maximum ice thickness (Fig. 8). Since the ice model overestimates the NID, it is more suitable to evaluate its change by computing a percentage compared to the baseline period. The NID can be expected to decrease by 9–19% under $RCP4.5_{near}$ and 9–22% under $RCP8.5_{near}$ (Table 5). The highest difference is computed using the data of ICHEC under $RCP8.5_{near}$, while the model that fit the observations the best (CNRM) showed a shortening NID by ~8.6% in the near future. In the far future the NID can be expected to shorten by 16–36% under $RCP4.5_{far}$ compared with the baseline run, while the highest change can be seen under $RCP8.5_{far}$, ranging from 46% to 67% less ice days.

In all climate model cases, the NID displayed a statistically significant decreasing trend ($p < 0.05$) for the period of 2006–2100, while during the baseline period it was not significant, apart from ICHEC ($p = 0.01$). During the baseline period the NID was decreasing with 0.55–2.39 days year^{-1}, while MPI showed an increasing rate of 0.22 days year^{-1} (Table 6). The decrease ranged from 0.17 to 0.53 days year^{-1} under RCP4.5, and 0.66–1.07 days year^{-1} under RCP8.5 scenario.

Discussion

In this paper, we presented a deterministic numerical modelling application for the ice thickness projections in the shallow freshwater lagoon, the Curonian Lagoon (CL). Our chosen ice thermodynamic model (by Tedesco *et al.*

Table 6. The decrease rate of mean and maximum ice thickness (cm year^{-1}), and number of ice days (NID, days year^{-1}) during the baseline period (BS, 1986–2005) and under RCP4.5 and RCP8.5 climate change scenarios of data from five climate models: ICHEC, CNRM, IPSL, MOHC, and MPI, over the period of 2006–2100.

	CNRM	ICHEC	IPSL	MOHC	MPI
Mean					
BS	–0.30	–0.91	–0.41	0.09	0.34
RCP4.5	–0.07	–0.06	–0.04	–0.07	–0.06
RCP8.5	–0.12	–0.05	–0.06	–0.08	–0.10
Max					
BS	–0.63	–1.32	–1.06	0.36	0.79
RCP4.5	–0.18	–0.13	–0.12	–0.15	–0.11
RCP8.5	–0.30	–0.11	–0.19	–0.23	–0.24
NID					
BS	–0.49	–2.39	–1.22	–0.55	0.22
RCP4.5	–0.53	–0.51	–0.36	–0.47	–0.17
RCP8.5	–0.92	–0.73	–1.07	–0.79	–0.66

2009, Tedesco *et al.* 2010) showed being suitable for ice thickness projections in a freshwater environment. We calibrated the ice thermodynamic model by testing various classes of snow density values, of which the best results gave the higher density model set-up. Higher snow density leads to higher heat conductivity of snow, resulting in an increased ice thickness (Zhao *et al.* 2019). The ice growth and melt patterns as well as thickness were simulated rather accurately in all three stations in the CL (mean RMSE = 0.06 m, R = 0.92). The average snow thickness correlation with the observations was strong in Nida and Juodkrantė, while in Ventė it was moderate. The model's ability to adequately simulate snow thickness highly depends on the meteorological forcing data. Model runs using local weather observations produced much better results.

Since snow is a very good insulator, the model sensitivity tests showed that thicker snow cover leads to slower ice growth, thus the bias in the snow thickness can lead to the bias of maximum ice thickness. However, precipitation rate is highly dependent on the air temperature. Overall ice parameters and air temperature have a linear relationship — decreasing air temperature extends the number of ice and snow days due to prolonged freezing period, likewise increasing the average ice and snow thickness.

Overall, the model represents the total ice thickness very well, and the number of simulated ice layers appears to be enough. Some other studies (Cheng *et al.* 2008, Lecomte *et al.* 2011) suggest that the increased vertical resolution of the model, e.g., by up to 15–20 layers, can improve the results. However, the same study of Cheng *et al.* (2008), stated that the accuracy of model forcing was much more important than the vertical resolution.

The number of ice days was highly overestimated by the model (on average by one month, ranging from 3 to 40 days), while the correlation with the observations was very strong (mean R = 0.95). The computation of common ice season duration from the freeze-up and melt-off dates, did not give good results compared to the observation data, due to short and very thin ice freezing events early in the beginning and sometimes at the end of the continuous ice cover, which were not recorded in the coastal observations. Eliminating these sporadic freezing events in the model data lead to the ice season duration values being much closer to that of observation data (mean R = 0.98, compared to R = 0.78 of uncorrected ice seasons).

The application of global climate model (GCM) projections in ice thermodynamic model revealed that global scale climate data have a very coarse resolution considering the small size of the Curonian Lagoon, and are not entirely suitable for such small-scale applications. Due to the higher air temperature the ice model during the baseline period mostly underestimated ice thickness compared to the present-day period (computed using observation data), thus GCM require downscaling and bias correction to fit the local climate. The downscaling approach is also often carried out for the modelling studies of larger domains, such as the Baltic Sea (Wibig *et al.* 2015), denoting the importance and benefits of high-resolution forcing data (Hermans *et al.* 2020).

The mean ice thickness in the CL could be expected to decrease by ~30% in the near future, having similar results under both RCP scenarios. By the end of the century, the average ice thickness will undergo drastic changes compared with the baseline period, decreasing by on average 60% under RCP4.5 and 85% under RCP8.5 scenarios. The maximum ice thickness can be expected to decrease by 40% in RCP4.5$_{far}$ and 60% in RCP8.5$_{far}$, while only 13–18% in the near future.

Our results correspond with another study of ice thickness projections using statistical methods by Jakimavičius *et al.* (2019), which showed that in the far future (RCP4.5$_{far}$), the average ice thickness will decline by 53% compared to the reference period of 1986–2005. However, they project that for RCP8.5$_{far}$, ice will form once every five years reaching 4–11 cm thickness, while in our projections the ice will form every year but the mean/max ice thickness would be only ~1/4cm. Although, this difference between our study and Jakimavičius *et al.* (2019), could also be due to different averaging periods (we averaged over Nov.–Apr. period) since the averaging period in their study is not specified.

The ice thickness around the Baltic Sea coastal areas does not show any consistent

trend in the baseline observations (Jevrejeva *et al.* 2004, Haapala *et al.* 2015). In the far future under RCP8.5, the area outside the Bay of Bothnia could be ice free and the mean annual maximum ice thickness is projected to decrease with a rate of 0.1–0.34 cm year^{-1} and 0.08–0.76 cm year^{-1} under RCP4.5 and RCP8.5, respectively, with higher values northward (Luomaranta *et al.* 2014). In our study, we project a decrease of maximum ice thickness with a rate of 0.11–0.18 cm year^{-1} under RCP4.5 and 0.11–0.30 cm year^{-1} under RCP8.5.

The NID can be expected to decrease by ~15% (five-model mean) in the near future under both RCP scenarios compared to the baseline data. Whilst in the far future this change could increase up to 30% under RCP4.5 and even 57% under RCP8.5. Translated to days this is decreasing from the average 130 days during the baseline period to 110 days in the near future and 92 days in RCP4.5$_{far}$ and 56 days in RCP8.5$_{far}$. However, since ice model overestimated the NID during the present-day period, these values are likely be lower.

The study of Jakimavičius *et al.* (2019) proposed that ice season would last 35–45 days and 3–34 days in the near and far future, respectively. Their study showed that ice duration is on average 55 days during the reference period (1986–2005), ranging from 17 to 87 days. However, the study of Idzelytė *et al.* (2019) showed that during 2002–2003 the ice season duration in the Curonian Lagoon was 123 days based on observation data, which is longer than the specified range of Jakimavičius *et al.* (2019). Jakimavičius *et al.* (2019) also used data from the station in Klaipėda Strait, where the ice usually does not form or is very thin and not land locked, due to the more saline water and intensive shipping. Therefore, it could be implied that the inclusion of data from the strait lead to underestimated values.

In the Baltic Sea, it is expected that the length of the ice season can decrease by 1–2 months in the northern parts and 2–3 months in the central parts (HELCOM 2007). Based on the baseline observations, the decrease is observed from east to west, and from the inner waters towards the sea areas (Haapala *et al.* 2015). In the small sheltered areas in the southern Baltic, e.g., Vistula lagoon, the duration of ice phenomenon is constantly decreasing, however with large irregularities (Majewski 2011). The decrease rate of NID during baseline period in our study is 0.88 days year^{-1} (five-model mean), which is higher than that reported in the study of Jakimavičius *et al.* (0.2 days year^{-1}), along the Lithuanian Baltic Sea coast (0.64 days year^{-1}; Dailidienė *et al.* 2012), along the Latvian coast and in the Gulf of Riga (~0.3 days year^{-1}) (Kļaviņš *et al.* 2016), the eastern Gulf of Finland (0.6 days year^{-1}; Ronkainen 2013), or in the lakes of northern Poland (0.54 days year^{-1}; Bartosiewicz *et al.* 2020).

Although with our study we do not project the ice cover to completely disappear from the Curonian Lagoon, the whole phenology will evidently undergo drastic changes to a shortened ice season duration and loss of thickness. These changes will affect the underwater environment by changes in the hydrodynamic (Idzelytė *et al.* 2020) and ecological (Potyutko 2018) regimes, the living conditions of the residents in coastal areas by decreasing the flooding events caused by ice jams, as well as disappearing winter recreational activities. The applied ice thermodynamic model still requires work to fit the overall observed ice season duration, e.g., inclusion of the varying speed of under-ice currents, mixed layer temperature, salinity data, likewise adjusting the freezing temperature, with possible additional experiments, such as application of a first-order analysis using simple analytic methods (Karetnikov *et al.* 2017). However, the ice thickness corresponded very well to the measurements and could be used as a guideline for future investigations.

Acknowledgements: The preparation of this paper was partially funded by European Social Fund (project no: 09.3.3-LMT-K-712-01-0178) under grant agreement with the Research Council of Lithuania (LMTLT).

References

Bartosiewicz M., Ptak M., Woolway R.I., Sojka M. 2020. On thinning ice: Effects of atmospheric warming, changes in wind speed and rainfall on ice conditions in temperate lakes (Northern Poland). *J. Hydrol.*: 125724, doi:

j.jhydrol.2020.125724.

Baukšys J. 1978. Ledo režimas [Ice regime]. In: Rainys A. (ed.), *Kuršių marios* [*The Curonian Lagoon]*, Vilnius, pp. 34–49. [In Lithuanian].

Börgel F., Frauen C., Neumann T. & Meier H.E.M. 2020. The Atlantic Multidecadal Oscillation controls the impact of the North Atlantic Oscillation on North European climate. *Environ. Res. Lett.* 15: 104025, doi: 10.1088/1748-9326/aba925.

Chassignet E. & Verron J. 1998. *Ocean Modeling and Parameterization*. Springer, Netherlands.

Cheng, B., Z. Zhang, T. Vihma, M. Johansson, L. Bian, Z. Li, and H. Wu (2008), Model experiments on snow and ice thermodynamics in the Arctic Ocean with CHINARE 2003 data. *J. Geophys. Res.* 113: C09020, doi:10.1029/2007JC004654.

Dailidienė I., Davulienė L., Kelpšaitė L., Razinkovas A. 2012. Analysis of the Climate Change in Lithuanian Coastal Areas of the Baltic Sea. *J. Coast. Res*. 28, 557–569, doi: 10.2112/JCOASTRES-D-10-00077.1.

EEA. 2017. *Climate change, impacts and vulnerability in Europe 2016. An indicator-based report*. Luxembourg, Publications Office of the European Union.

Fallis A.G. 2018. Global Warming of 1.5°C. An IPCC Special Report on the impacts of global warming of 1.5°C above pre-industrial levels and related global greenhouse gas emission pathways, in the context of strengthening the global response to the threat of climate change. *J. Chem. Inf. Model*. 53(9): 3–25.

George G. 2010. *The Impact of Climate Change on European Lakes*. Springer Netherlands.

Girjatowicz J.P. 2005. The Relationships Between the North Atlantic Oscillation and Southern Baltic Coast Ice Conditions. *J. Coast. Res.* 212: 281–291, doi: 10.2112/03-0073.1.

Haapala J.J., Ronkainen I., Schmelzer N. & Sztobryn M. 2015. Recent Change – Sea Ice. In: The BACC II Author Team (eds.), *Second Assessment of Climate Change for the Baltic Sea Basin, Regional Climate Studies*, Springer International Publishing, Cham, pp. 145–153.

HELCOM 2007. Climate Change in the Baltic Sea Area –- HELCOM Thematic Assessment in 2007. *Balt. Sea Environ. Proc.* No. 111, 54.

HELCOM, 2013 Climate change in the Baltic Sea Area: HELCOM thematic assessment in 2013. *Balt. Sea Environ. Proc.* No. 137.

Herman A., Jedrasik J. & Kowalewski M. 2011. Numerical modelling of thermodynamics and dynamics of sea ice in the Baltic Sea. *Ocean Sci*. 7: 257–276, doi: 10.5194/os-7-257-2011.

Hermans T.H.J., Tinker J., Palmer M.D., Katsman C.A., Vermeersen B.L.A. & Slangen A.B.A. 2020. Improving sea-level projections on the Northwestern European shelf using dynamical downscaling. *Clim. Dyn.* 54: 1987–2011, doi:10.1007/s00382-019-05104-5.

Hersbach H., Bell B., Berrisford P., Biavati G., Horányi A., Muñoz Sabater J., Nicolas J., Peubey C., Radu R., Rozum I., Schepers D., Simmons A., Soci C., Dee D., Thépaut J-N. 2018. ERA5 hourly data on single levels from 1979 to present. Copernicus Climate Change Service (C3S) Climate Data Store (CDS). (Accessed on < 15-Nov-2020 >), doi: 10.24381/cds.adbb2d47.

Hunke E.C., Lipscomb W.H. & Turner A.K. 2011. Sea-ice models for climate study: Retrospective and new directions. *J. Glaciol.* 56: 1162–1172, doi: 10.3189/002214311796406095.

Idzelytė R., Kozlov I.E. & Umgiesser G. 2019. Remote Sensing of Ice Phenology and Dynamics of Europe's Largest Coastal Lagoon (The Curonian Lagoon). *Remote Sens.* 11, 2059, doi: 10.3390/rs11172059.

Idzelytė R., Mėžinė J., Zemlys P. & Umgiesser, G. 2020. Study of ice cover impact on hydrodynamic processes in the Curonian Lagoon through numerical modeling. *Oceanologia*, 62: 428–442 doi: 10.1016/j.oceano.2020.04.006.

IPCC. 2013. *Climate Change 2013: The Physical Science Basis. Contribution of Working Group I to the Fifth Assessment Report of the Intergovernmental Panel on Climate Change.* Stocker T.F., Qin D., Plattner G.K., Tignor M., Allen S.K., Boschung J., Nauels A., Xia Y., Bex V. & Midgley P.M. (eds.), Cambridge University Press, Cambridge, United Kingdom and New York, NY, USA, 1535 pp.

IPCC. 2019. Technical Summary. In: Pörtner H.O., Roberts D.C., Masson-Delmotte V., Zhai P., Poloczanska E., Mintenbeck K., Tignor M., Alegría A., Nicolai M., Okem A., Petzold J., Rama B. & Weye N.M. (eds.), *IPCC Special Report on the Ocean and Cryosphere in a Changing Climate*. [In press.].

Jakacki J. & Meler, S. 2019. An evaluation and implementation of the regional coupled ice-ocean model of the Baltic Sea. *Ocean Dyn.* 69: 1–19, doi: 10.1007/s10236-018-1219-8.

Jakimavičius D., Šarauskienė D. & Kriaučiūnienė J. 2019. Influence of climate change on the ice conditions of the Curonian Lagoon. *Oceanologia* 62: 164–172, doi: 10.1016/j.oceano.2019.10.003.

Jevrejeva S., Drabkin V.V., Kostjukov J., Lebedev AA., Leppäranta M., Mironov Y.U., Schmelzer N. & Sztobryn M. 2004. Baltic Sea ice seasons in the twentieth century. *Clim. Res.* 25: 217–227, doi: 10.3354/cr025217.Kendall M.G. & Gibbons J.D. 1990. *Rank Correlation Methods*. Edward Arnold, London, UK.

Karetnikov S., Leppäranta M. & Montonen A. 2017. A time series of over 100 years of ice seasons on Lake Ladoga. *J. Great Lakes Res.*, *43*(6), 979–988, doi: 10.1016/j.jglr.2017.08.010.

Kendall M.G. & Gibbons J.D. 1990. *Rank Correlation Methods*. Edward Arnold, London, UK.

Kļaviņš M., Avotniece Z. & Rodinovs V. 2016. Dynamics and Impacting Factors of Ice Regimes in Latvia Inland and Coastal Waters. *Proc. Latv. Acad. Sci. Sect. B. Nat. Exact, Appl. Sci.* 70: 400–408, doi: 10.1515/prolas-2016-0059.

Kozlov I.E., Krek E.V., Kostianoy A.G. & Dailidienė I. 2020. Remote Sensing of Ice Conditions in the Southeastern Baltic Sea and in the Curonian Lagoon and Validation of SAR-Based Ice Thickness Products. *Remote Sens.* 12: 3754, doi: 10.3390/rs12223754.

Lecomte, O., Fichefet, T., Vancoppenolle, M., Nicolaus, M.,

2011. A new snow thermodynamic scheme for large-scale sea-ice models. Ann. Glaciol. 52, 337–346, doi: 10.3189/172756411795931453.

Lenderink G., Buishand A. & Van Deursen W. 2007. Estimates of future discharges of the river Rhine using two scenario methodologies: Direct versus delta approach. *Hydrol. Earth Syst. Sci.* 11: 1145–1159, doi: 10.5194/hess-11-1145-2007.

Leppäranta M. & Myrberg K. 2009. *Physical Oceanography of the Baltic Sea*. Springer-Praxis, Chichester.

Luomaranta A., Ruosteenoja K., Jylhä K., Gregow H, Haapala J. & Laaksonen A. 2014. Multimodel estimates of the changes in the Baltic Sea ice cover during the present century. *Tellus A*. 66: 22617, doi: 10.3402/tellusa.v66.22617.

Majewski W. 2011. Ice Phenomena on the Lower Vistula. *Geophysica* 47: 57–67.

Martin J. & McCutcheon S. 1999. *Hydrodynamics and Transport for Water Quality Modeling*. Boca Raton, CRC Press.

Omstedt A. & Wettlaufer J.S. 1992. Ice growth and oceanic heat flux: Models and measurements. *J. Geophys. Res. Ocean.* 97: 9383–9390, doi: 10.1029/92JC00815.

Pedersen R.A., Cvijanovic I., Langen P.L. & Vinther B.M. 2016. The Impact of Regional Arctic Sea Ice Loss on Atmospheric Circulation and the NAO. *J. Clim.* 29: 889–902, doi: 10.1175/JCLI-D-15-0315.1

Pemberton P., Löptien U., Hordoir R., Höglund A., Schimanke S., Axell L. & Haapala J. 2017. Sea-ice evaluation of NEMO-Nordic 1.0: a NEMO-LIM3.6-based ocean-sea-ice model setup for the North Sea and Baltic Sea. *Geosci. Model Dev*. 10: 3105–3123, doi: 10.5194/gmd-10-3105-2017.

Peng G., Matthews J.L., Wang M., Vose R. & Sun, L. 2020. What Do Global Climate Models Tell Us about Future Arctic Sea Ice Coverage Changes? *Climate* 8, 15, doi: 10.3390/cli8010015.

Potyutko, O.M. 2018. Impact of Seasonal Ice on the Structure of the Dreissena polymorpha (Pallas, 1771) Beds in the Swash-Ice Zone of the Curonian Lagoon and the Peculiarities of Formation of the Zebra-Mussel Bed. *Inland Water Biol* 11**:** 337–343, doi: 10.1134/S199508291803015X.

Randall D.A., Wood R.A., Bony S., Colman R., Fichefet T., Fyfe J., Kattsov V., Pitman A., Shukla J., Srinivasan J., Stouffer R.J., Sumi A., Taylor K.E. 2007. Cilmate Models and Their Evaluation. In: Solomon S., Qin D., Manning M., Chen Z., Marquis M., Averyt K.B., Tignor M., Miller H.L. (eds.), *Climate Change 2007: The Physical Science Basis. Contribution of Working Group I to the Fourth Assessment Report of the Intergovernmental Panel on Climate Change*, Cambridge University Press, Cambridge, United Kingdom and New York, NY, USA.

Ronkainen I. 2013. *Long-Term Changes in Baltic Sea Ice Conditions*. University of Helsinki, Finland. [Master's Thesis].

Rukšėnienė V., Dailidienė I., Myrberg K. & Dučinskas K. 2015. Simple approach for statistical modelling of ice phenomena in the curonian lagoon, the south-eastern Baltic Sea. *Baltica* 28: 11–18, doi: 10.5200/baltica.2015.28.02

Sharma S., Blagrave K., Magnuson J.J., O'Reilly C.M., Oliver S., Batt R.D., Magee M.R., Straile D., Weyhenmeyer G.A., Winslow L. & Woolway R.I. 2019. Widespread loss of lake ice around the Northern Hemisphere in a warming world. *Nat. Clim. Chang.* 9, 227–231, doi: 10.1038/s41558-018-0393-5.

Simon A., Frankignoul C., Gastineau G., & Kwon Y. 2020. An Observational Estimate of the Direct Response of the Cold-Season Atmospheric Circulation to the Arctic Sea Ice Loss. *J. Clim. 33*: 3863–3882, doi: 10.1175/jcli-d-19-0687.1.

Stroeve J.C., Serreze M.C., Holland M.M., Kay J.E., Malanik J. & Barrett A.P. 2012. The Arctic's rapidly shrinking sea ice cover: a research synthesis. *Clim. Change* 110: 1005–1027, doi: 10.1007/s10584-011-0101-1.

Tedesco L. 2009. *Modelling coupled physical-biogeochemical processes in ice-covered oceans*. University of Bologna, Italy. [PhD Thesis].

Tedesco L., Vichi M., Haapala J. & Stipa T. 2009. An enhanced sea-ice thermodynamic model applied to the Baltic Sea. *Boreal Environ. Res.* 14: 68–80.

Tedesco L., Vichi M., Haapala J. & Stipa T. 2010. A dynamic Biologically Active Layer for numerical studies of the sea ice ecosystem. *Ocean Model.* 35: 89–104, doi: 10.1016/j.ocemod.2010.06.008.

Umgiesser G., Zemlys P., Erturk A., Razinkovas-Baziukas A., Mezine J. & Ferrarin C. 2016. Seasonal renewal time variability in the Curonian Lagoon caused by atmospheric and hydrographical forcing. *Ocean Sci.* 12: 391–402, doi: 10.5194/os-12-391-2016.

Vihma T. 2014. Effects of Arctic Sea Ice Decline on Weather and Climate: A Review. *Surv. Geophys.* 35: 1175–1214, doi: 10.1007/s10712-014-9284-0.

Vihma T. & Haapala J. 2009. Geophysics of sea ice in the Baltic Sea: A review. *Prog. Oceanogr.* 80: 129–148, doi: 10.1016/j.pocean.2009.02.002.

Wibig J., Maraun D., Benestad R., Kjellström E., Lorenz P. & Christensen O.B. 2015. Projected Change –- Models and Methodology. In: The BACC II Author Team (eds.), *Second Assessment of Climate Change for the Baltic Sea Basin. Regional Climate Studies*, Springer, Cham, doi: 10.1007/978-3-319-16006-1_10.

Wunderling N., Willeit M., Donges J.F. & Winkelmann R. 2020. Global warming due to loss of large ice masses and Arctic summer sea ice. *Nat. Commun.* 11: 5177, doi: 10.1038/s41467-020-18934-3.

Yadav J., Kumar A. & Mohan R. 2020. Dramatic decline of Arctic sea ice linked to global warming. *Nat Hazards.* 103: 2617–2621, doi: 10.1007/s11069-020-04064-y.

Yu Karpechko A., Peterson K.A., Scaife A.A., Vainio J. & Gregow H. 2015. Skilful seasonal predictions of Baltic Sea ice cover. *Environ. Res. Lett.* 10, 044007, doi: 10.1088/1748-9326/10/4/044007.

Zemlys P., Ferrarin C., Umgiesser G., Gulbinskas S. & Bellafiore D. 2013. Investigation of saline water intrusions into the Curonian Lagoon (Lithuania) and two-layer flow in the Klaipeda Strait using finite element hydro-

dynamic model. *Ocean Sci.* 9: 573–584, doi: 10.5194/os-9-573-2013.

Zhao, J., Cheng, B., Vihma, T., Yang, Q., Hui, F., Zhao, B., Hao, G., Shen, H., Zhang, L., 2019. Observation and thermodynamic modeling of the influence of snow cover on landfast sea ice thickness in Prydz Bay, East Antarctica. Cold Reg. Sci. Technol. 168, 102869. https://doi.org/10.1016/j.coldregions.2019.102869.